Gain Measurements of Fabry-Pérot InP/InGaAsP Lasers using an Ultra High Resolution Spectrometer

Y. Barbarin, E.A.J.M Bente, G. Servanton, L. Mussard, Y.S. Oei, R. Nötzel and M.K. Smit

COBRA, Eindhoven University of Technology, Den Dolech 2, P.O. Box 513, 5600 MB, Eindhoven, The Netherlands

Abstract: We present for the first time measurements of the optical gain in a semiconductor laser using a 20 MHz resolution optical spectrum analyzer. The high resolution allows for accurate gain measurements close to the lasing threshold. This is demonstrated by gain measurements on a bulk InGaAsP 1.5 μm Fabry-Perot laser. Combined with direct measurement of transparency carrier density values, parameters were determined for characterizing the gain at a range of wavelengths and temperatures. The necessity of the use of a logarithmic gain model is shown.

OCIS codes :

250.5980 Semiconductor optical amplifiers

300.6320 Spectroscopy, high-resolution

140.5960 Semiconductor lasers

130.3130 Integrated optics materials

Introduction

The optical gain in a semiconductor laser is an essential parameter to characterize fabricated lasers and to simulate their behavior. The most commonly used method to measure the gain in laser cavities is the so called Hakki-Paoli method [1]. In this method the optical gain is derived from the contrast ratio of the modulations in the spectrum of the Amplified Stimulated Emission (ASE) caused by the resonances of the laser cavity operating below threshold. The main advantage of this method is that no external source, wideband antireflection coating of the laser facets or accurate values of the coupling efficiency are required. This intensively used method is however sensitive to noise and its results are significantly influenced by the response function of the spectrometer. Cassidy was first to improve the method by introducing a ratio between the integral of the intensity of a mode peak and the minimum intensity [2]. This makes the method less sensitive to the resolution of the Optical Spectrum Analyzer (OSA) however both methods are still sensitive to the noise. Wang and Cassidy have recently proposed and demonstrated a method using a non-linear least-squares fitting of the Fabry-Pérot equation which is less sensitive to noise [3]. By taking into account all the data points of the spectrum, it improves the accuracy as compared to previous methods. However they had to introduce a correction to take into account the finite line-width of the OSA. In this paper we present measurements done using an ultra high resolution OSA (20 MHz ~0.16pm). Thus the effect of the response function of the OSA does not need to be compensated. Such high resolution provides a very good accuracy in the gain measurement right up to the threshold of the laser.

Also the cavity of the lasers under investigation can be longer than 1mm which is the typical limit for standard grating based OSAs. This can be an issue with devices with low gain, such as quantum dot lasers, or lasers in larger integrated circuits. We demonstrate the high accuracy method and combine it with measurements of the optical transparency point by determining the optical gain spectrum and the differential gain of an InP/InGaAsP Fabry-Pérot laser structure as a function of injected carrier density. Results for a range of heat sink temperatures around room temperature are presented. These parameters will be used in our simulation models for lasers fabricated with identical layer stacks.

Gain measurement method

The steady-state optical output spectrum of a Fabry-Pérot laser below threshold is described by the following Airy function equation [4].

$$I(\lambda) = B(\lambda).\frac{\left(1+R.G\right)\cdot\left(1-R\right)}{\left(1-R.G\right)^2 + 4.R.G.\sin^2\left(\frac{2\pi.Ng.L}{\lambda}\right)} \tag{1}$$

Where $B(\lambda)$ is the total amount of spontaneous emission represented by an equivalent input flux, $G(\lambda)$ is the single-pass modal gain, R is the laser facet reflectivity, L is the cavity length and Ng is the group index of the waveguide. The equation is rewritten and a background level is added to obtain an equation that is to be fitted to each mode peak in the recorded subthreshold ASE spectrum (2). No convolution with the OSA response is necessary.

$$I_{fit}(\lambda) = \frac{C}{\left(1-R\cdot G\right)^2 + 4\cdot R\cdot G\cdot\sin^2\left(2\cdot\pi\cdot Ng\cdot L\left(\frac{1}{\lambda}-\frac{1}{\lambda_{peak}}\right)\right)} + BKG \tag{2}$$

Where $R{\cdot}G(\lambda)=R{\cdot}G(\lambda_{peak}) + \gamma (\lambda - \lambda_{peak})$, $C(\lambda) = B(\lambda)(1 + P_{RG}(\lambda)) (1 - R) = C (\lambda_{peak}) +\beta (\lambda - \lambda_{peak})$, λ_{peak} is the peak wavelength of the individual mode, BKG is the background level. We assume that the spontaneous emission $B(\lambda)$ and the single pass gain $G(\lambda)$ vary linearly with wavelength over one mode. Thus, the small asymmetry of the Fabry-Pérot modes due to the change of the gain and ASE intensity with wavelength over the fitted range of approximately one free spectral range of the laser cavity is taken into account. The fitting is done in a Matlab program using the weighted non-linear least-squares fitting function *lsqnonlin* from the optimization toolbox. First a scan over the measured spectra is performed to extract starting values for $\lambda peak$ and *BKG*. Since the spectrometer also provides accurate frequency/wavelengths differences between the mode peak positions, the group index $Ng(\lambda)$ is calculated on the different λ_{peak} by using this formula: $Ng((\lambda_{peak}^{i+1}+\lambda_{peak}^{i}) / 2) = (\lambda_{peak}^{i+1}+\lambda_{peak}^{i})^2 / (8.(\lambda_{peak}^{i+1}-\lambda_{peak}^{i}).L)$. The group index as a function of wavelength is then fitted over the total spectral range using the Cauchy formalism: $Ng(\lambda) = N_0 + N_1 / \lambda^2$. The fitting parameters in the airy function are therefore C, P_{RG}, β, γ, BKG and λ_{peak}. The weights used for the data points are defined in equation (3).

$$weight(\lambda) = \frac{1}{\sqrt{(\varepsilon.I(\lambda))^2 + \sigma^2_{BKG}}} \tag{3}$$

$I(\lambda)$ is the measured signal intensity and σ_{BKG} the standard deviation of the background signal is determined from areas in spectrum with a very low signal intensity. The parameter ε is chosen in order to minimize the residue of the fit. Tests have been performed for different spectrum intensities and InP based lasers. Results show that a clear reduction of the residue of

the fit is obtained for low intensity signal $\varepsilon = 0.15 \pm 0.02$. The effect of ε is minor for signal closer to the threshold.

Gain curve measurements

The measurements were performed on a Fabry-Pérot InP/InGaAsP ridge waveguide laser on an InGaAsP chip that was fixed onto a temperature controlled copper mount. The laser output is coupled into a lensed fiber and led through an optical isolator to the high resolution OSA (APEX AP2041A). The OSA is based on a heterodyne receiver principle using a single mode tunable laser as a local oscillator which enables the achievement of a resolution of 0.16 pm (20 MHz) and a wavelength accuracy of ± 3pm. The spectra were recorded in sections of 5 nm (20.000 points each) in order to have the full resolution available over the full wavelength range of interest. All the measurements were performed below the lasing threshold. No polarizer has been required as the polarization has been measured to be TE (30dB polarizer extinction).

The laser layer stack consists of a 120 nm thick $\lambda = 1.5$ µm bulk InGaAsP layer between two 190nm thick $\lambda = 1.25$ µm InGaAsP layers. The structure is clad by a 1500-nm thick p-InP layer with gradual doping levels and a 50 nm p-InGaAs contact layer. The cavity is 1985 µm long and the waveguide is 2 µm wide. The threshold is around 92 mA at 16°C and around 113 mA at 28°C. As can be seen in figure 1 the cavity modes are very well resolved in this typical ASE spectrum. The result of a typical fit over three modes is presented in figure 2. The spectrometer fully resolves the modes which are easily fitted with an appropriate weighting of the data.

Once all the modes in the spectra are fitted, R•G products can be plotted versus the wavelength for each injected current value. Results for T= 16°C and T=28°C are plotted in figures 3a and 3b. The typical gain shape is observed [5]. Very few observed modes did not lead

to a good fit (<1%). This happened when an excess of noise is detected during the measurement. Those points are removed from further calculations on the gain curves. The gain peak shifts over 8.0 nm from 16°C to 28°C. The gain peak wavelength shifts to the smaller values with an increase in carrier density as expected. The temperature appears to have an effect on the shape of the gain spectrum on the short wavelength side. To bring out the difference in bandwidth observed at the two temperatures, the gain spectra recorded at 16°C and 28°C are combined in figure 4. The gain spectra have been averaged over 1 nm (~6 modes) to reduce the noise. The gain maxima of the data at the two temperatures have been overlayed to illustrate that the bandwidth increases slightly with temperature by about 3 nm at the FWHM.

Discussion of the method

Measurements of the gain curves using the high resolution spectrometer gave smooth curves for RG product values higher than 0.4, below this value RG products becomes inaccurate. The high resolution inexorably limits the sensitivity of the equipment. The sensitivity of the instrument is specified for -75 dBm. However level down to -85dBm has been measured. On the other hand, high quality measurements are obtained at current values very close to the lasing spectrum. Wang and Cassidy have reported in [3] that the quality of their fitting of the modes became poor in the valleys in the gain regime where RG came close to 1. In order to improve the fit, they tried to change the weighting. Performing the fit to the logarithm of the convolution of the airy function and thereby significantly increasing the weight of the lower values data points, as well as including their instrument response function, did improve their results. However they could not successfully fit to values of the RG product close to and over 0.95. We have, using the high resolution spectrometer, been able to fit on the experimental data RG products up to 0.975 using weighting as given in equation 3, while maintaining an excellent agreement of the

measured and fitted laser modes. Figure 5 shows on a logarithmic scale the results of the fit of 3 modes compared with the experimental data. The RG product is around 0.972 for the three modes. All the measured points of the mode peaks are distributed well on both sides of the fitted curve. We observed that above the laser threshold the measured optical mode becomes wider, and can no longer be fitted using the Airy function as is to be expected. The extracted RG products are clamped to 0.99 and the shape of the mode starts to deviate from the airy function. This is illustrated in figure 6 where a measured and a fitted mode are shown at 1 mA above threshold.

Differential gain measurement

From the previously measured gain curves, the differential gain could be extracted. To improve the accuracy of the extracted differential gain per carrier, the gain curves have been smoothed over 6 modes (~ 1.0 nm). The net modal gain (g_{net}) per meter for each wavelength was then calculated using equation (4). This net gain is equal to the material gain g_m times the confinement factor Γ minus the total optical losses of the cavity α_{loss} which are comprised of the free carrier absorption within the active region and losses due to scattering.

$$g_{net} = \frac{1}{L} \cdot \mathbf{ln}\left(\frac{RG}{R}\right) = \Gamma \cdot g_m - \alpha_{loss} \tag{4}$$

To determine the differential gain a relation between the injected current and the carrier density is required. Below the laser threshold N can be extracted from the simplified rate equation (5).

$$\frac{N}{\tau} + B.N^2 + C.N^3 = \frac{I}{q \cdot S_{ActiveLayer} \cdot L} \tag{5}$$

Here τ is the carrier lifetime, B is the bimolecular recombination coefficient, C is the Auger recombination coefficient, I is the injected current, q is the charge of the electron, $S_{ActiveLayer}$ is the cross-section surface of the active layer of the SOA and L is the length of the SOA. All the values of the parameters used are listed in table 1.

A contour plot of the net optical modal gain as a function of carrier density and wavelength is presented in figure 7. From this figure one can see that the net modal gain at one wavelength varies non-linearly with the carrier density, even over this small range of carrier densities. This is most pronounced at the shortest wavelength in the plot. A common description for the relation between the material gain and the number of carriers is given below [6].

$$g_m = \alpha N \cdot N_0 \cdot \ln\left(\frac{N}{N_0}\right) \tag{6}$$

Here αN is the differential gain factor, N is the carrier density and N_0 is the transparency carrier density. The carrier density at transparency needs to be known for each wavelength and temperature. This was done by injecting light from a tunable laser (Agilent 81600B) that was modulated on/off at 1 kHz. The average power injected into the laser was – 13 dBm. The current of the laser under test is then scanned and the amplitude and phase of the modulation of the voltage over the laser as a result of the modulated input light is recorded using a lock-in amplifier. At the transparency current the interaction of the input light with the gain material should be minimal and the amplitude of the modulation is at a minimum. A clear jump in the phase of the modulation is also observed at the transparency point as the interaction of the laser light with the gain material changes from absorption to amplification. An example of an amplitude and phase signal from the lock-in amplifier is presented in figure 8. In this way we have measured the transparency current for 12, 20 and 28°C and for wavelengths between 1510

and 1590 nm. The carrier densities were calculated from the measured current using equation 5. The results are presented in figure 9 for different 3 temperatures. The transparency carrier density decreases almost linearly with the wavelength and increases significantly with temperature (~$8.4 \cdot 10^{21} \cdot m^{-3}$ per degree). To obtain values of the transparency carrier densities required in the differential gain calculation for wavelength values in the studied range and temperature, the presented graphs have been interpolated.

The discrete differential of the material gain (dg_m/dN) is calculated in order to extract $\alpha N(\lambda)$ without knowing the optical losses (7). Once the differential gain factor is known one can extract the internal losses from equation (4).

$$\frac{\partial g_m}{\partial N} = \frac{\partial}{\partial N}\left(\frac{1}{L \cdot \Gamma} \cdot \ln\left(\frac{RG(N,\lambda)}{R}\right)\right) = \alpha N \cdot \frac{N_0}{N} \tag{7}$$

Figure 10 shows the results of the differential gain from two temperatures (16°C and 28°C). We observed that at a fixed temperature, the differential gain as well as the transparency carrier density, decreases linearly with the wavelength over the observed wavelength range. Indicated in figure 10 are the wavelengths at which the device starts lasing for both temperatures which indicates the maximum modal gain. This graph has to be interpreted together with the transparency carrier density graph for different wavelength and temperatures (figure 9). With an increase of temperature, the maximum modal gain shifts to longer wavelengths. The transparency carrier density increases with temperature and this rise is larger for the shortest wavelengths. Meanwhile the differential gain increases with temperature as well. We observed that the slope of the linear fits decreases slightly with temperature and that the differential gain is lower at the maximum gain. Values reported here are higher than typical values reported in the literature for bulk InP/InGaAsP material [7-9]. This difference stems from the definition that we

have used for this parameter. The values listed here are the differential gains at the transparency density. The carrier density at laser threshold is typically significantly higher in order to overcome the mirror losses. If a linear gain model is used to describe the gain in a laser, the differential gain parameter is usually determined near the laser threshold. Looking at (6) one can see that a lower value of the differential gain parameter in the linear gain model is to be expected.

Once the differential gain is known, the losses could be calculated. Values for 16°C are -32dB/cm and values for 28°C are -33dB/cm. We attribute this increase in losses with temperature to the higher carrier concentration needed in the semiconductor at higher temperature.

Conclusion

We have demonstrated the use of an ultra-high resolution (20 MHz) spectrometer to accurately record subthreshold ASE spectra from a Fabry-Pérot InP/InGaAsP laser and determine the optical gain. The method is based on a non-linear least-squares fitting of the observed modes. The spectrometer fully resolves the modes which could be fitted accurately and the effect of the response function of the OSA does not need to be compensated for. Also it does not limit the measurement of devices shorter than 1 mm which is a typical limit for a standard spectrometer in this wavelength range. Measurements have been performed on a 2 mm long device and RG products up to 0.975 have been measured without any discernable difference between the measured and fitted laser modes. It has been observed that nearer to and above the lasing threshold the shape of the mode deviates from the Airy function and cannot be fitted. The optical gain spectrum of the laser has been measured successfully for different temperatures and subthreshold current values. The net gain curves obtained confirm the necessity of using the

logarithmic relation between gain and carriers. The differential gain parameter in the gain relation has been determined using measured transparency carrier density values for each wavelength and temperature. The parameters determined in this paper will be used in our laser simulation models.

Acknowledgments

This research is supported by the NRC Photonics program and the Towards Freeband Communication Impulse program of the Dutch Ministry of Economic Affairs.

Tables

Table 1. Values of the parameters used for the carrier density calculation.

Parameter	Description	Value used
Γ	Confinement factor	0.285
τ	Carrier lifetime	600 ps
B	Bimolecular recombination coefficient	$2.62.10^{-16}$ $m^3.s^{-1}$
C	Auger recombination coefficient	$5.269.10^{-41}$ $m^6.s^{-1}$
$S_{ActiveLayer}$	Surface of the active region	0.12x2 µm²
L	Length of the cavity	1.85 mm

List of figure captions

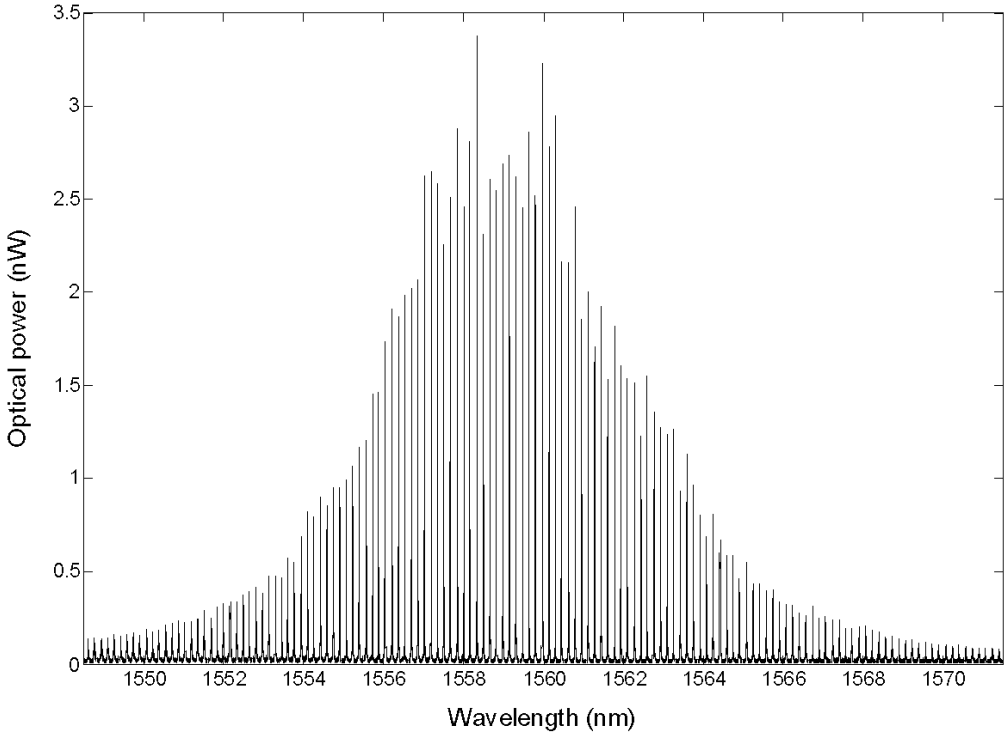

Figure 1. Typical example of a recorded subthreshold spectrum of a Fabry-Perot laser on a full span range. T=16°C I=89mA.

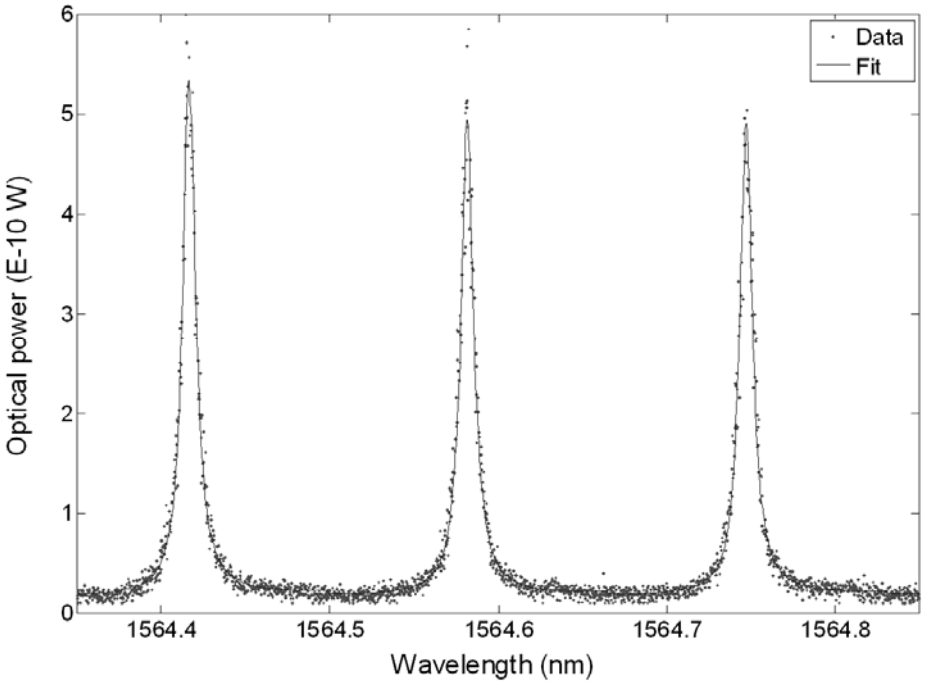

Figure 2. Measured and fitted spectra zoomed on three modes. T=16°C I=89mA.

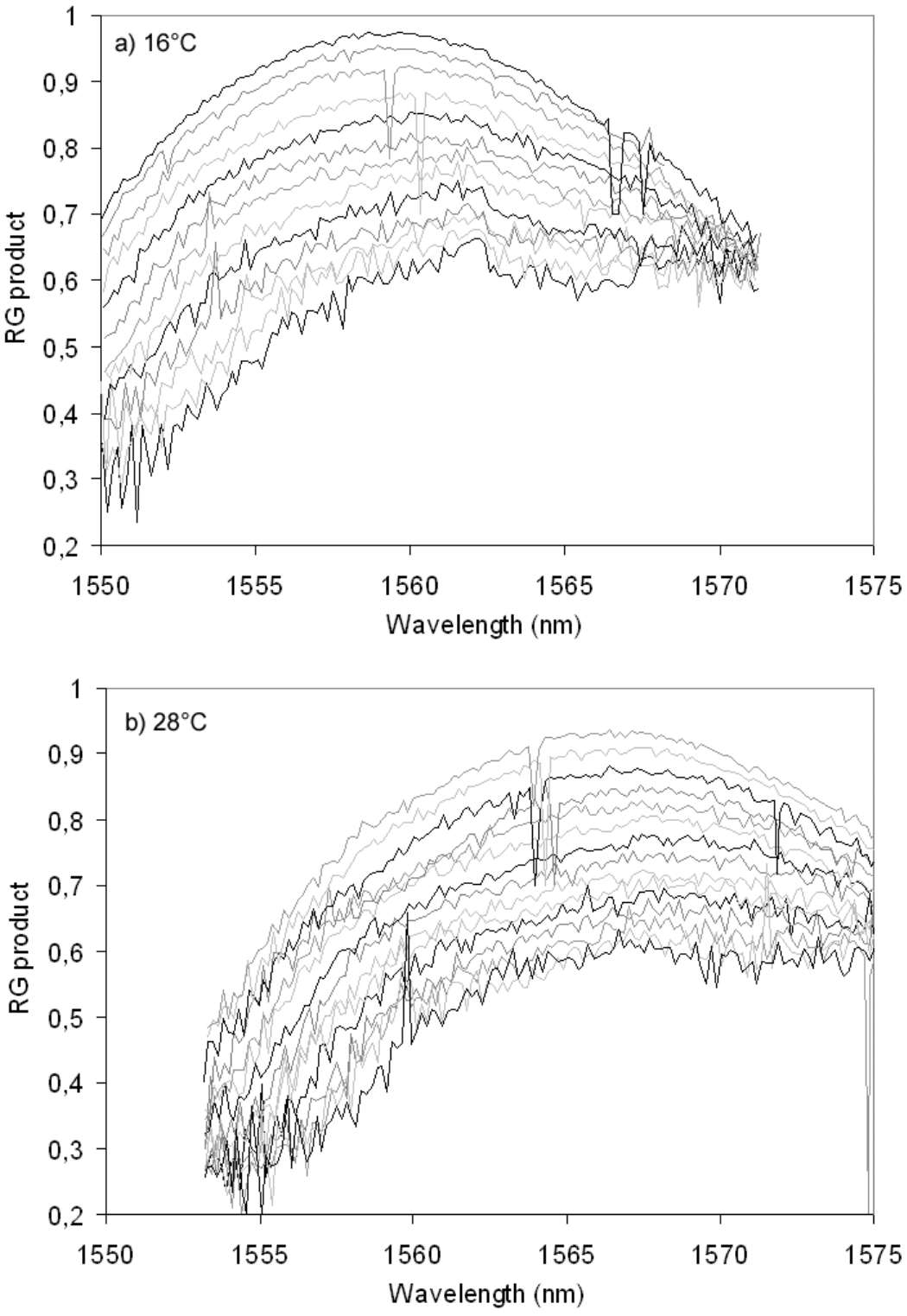

Figure 3. The *RG* product versus the wavelength and current in the SOA for a) T = 16°C b) T = 28°C

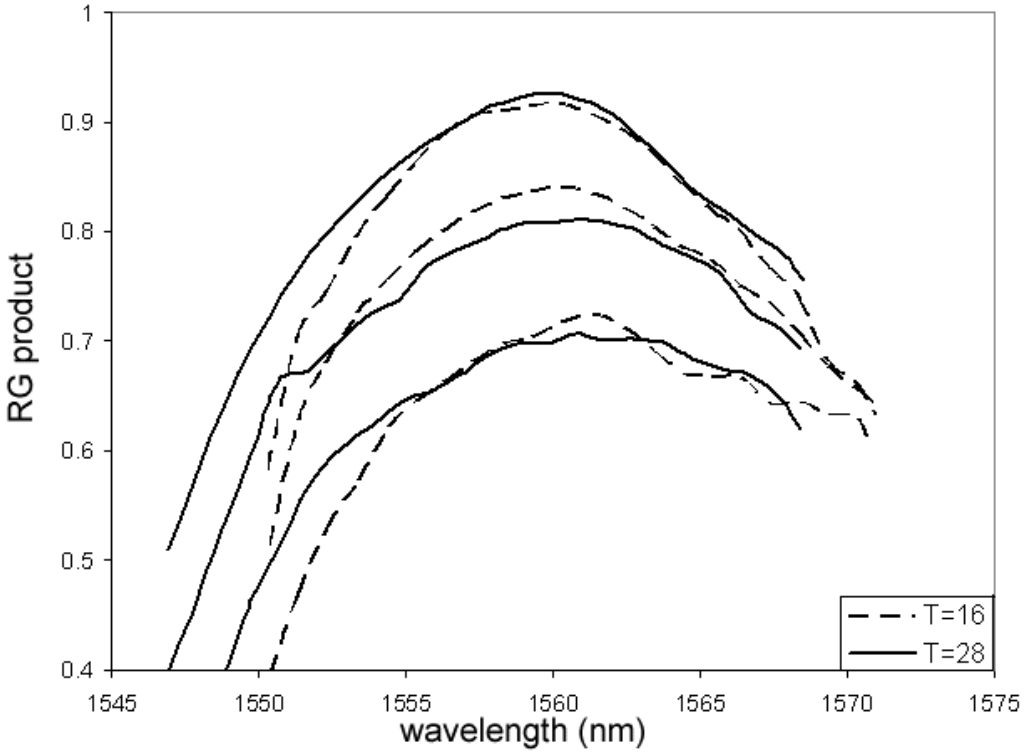

Figure 4. *RG* product for two temperature 16°C and 28°C and 3 similar RG values. The spectra for T=28°C has been shifted by 8 nm to better see the changes in shape.

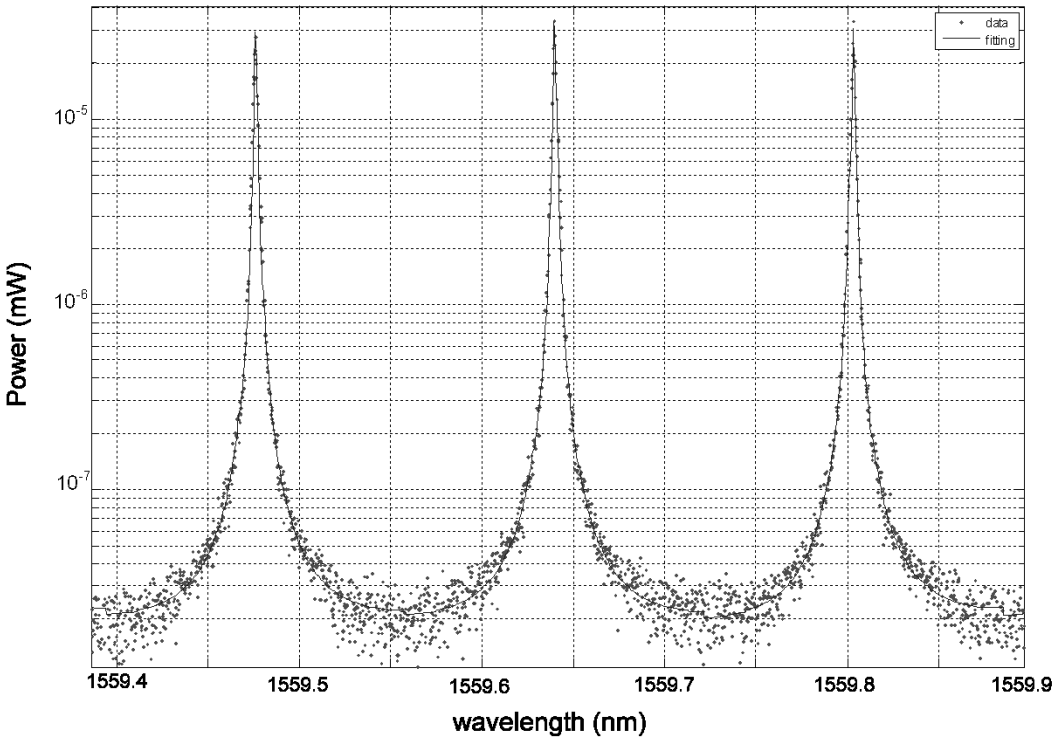

Figure 5. Measured and fitted spectra zoomed on three modes. T=16°C I=90mA. The three modes are perfectly fitted.

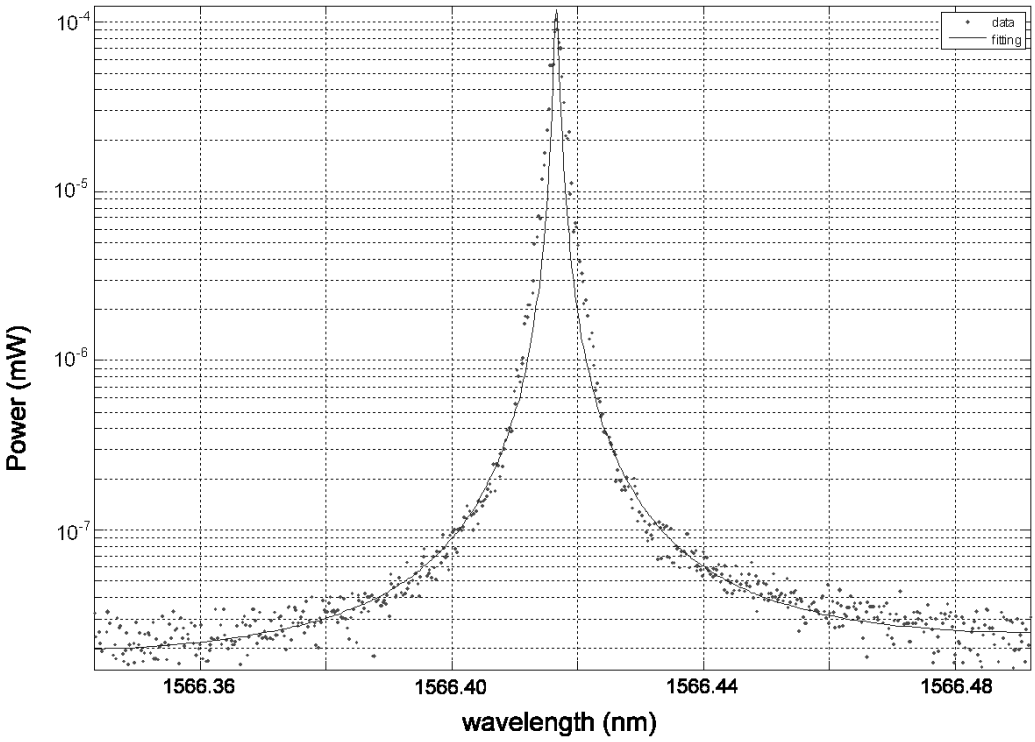

Figure 6. Measured and fitted spectra zoomed on a single mode. T=28°C I=114 mA. This is 1 mA above threshold, the Airy function is not valid anymore.

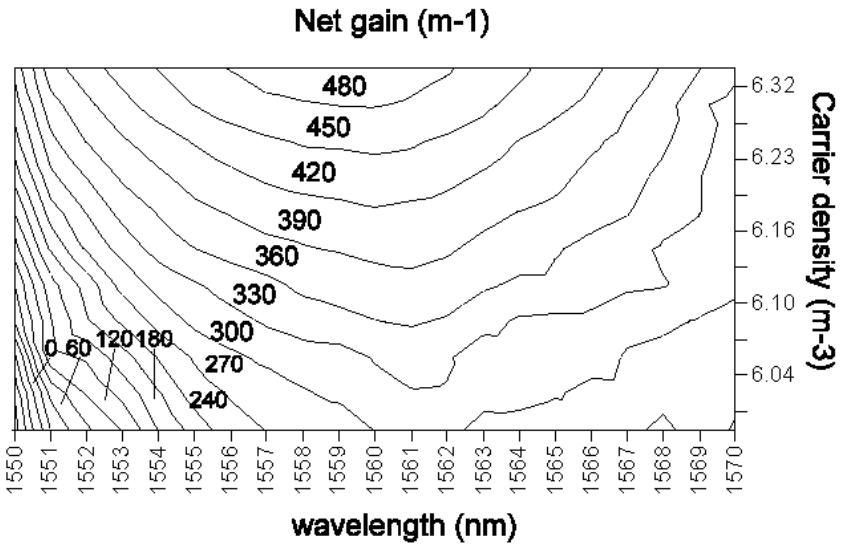

Figure 7. Contour plot of the measured net optical modal gain in the laser as a function of carrier density and wavelength at T = 16°C. At a fixed wavelength one can see that the gain does not increase linearly with carrier density, especially at the shorter wavelengths.

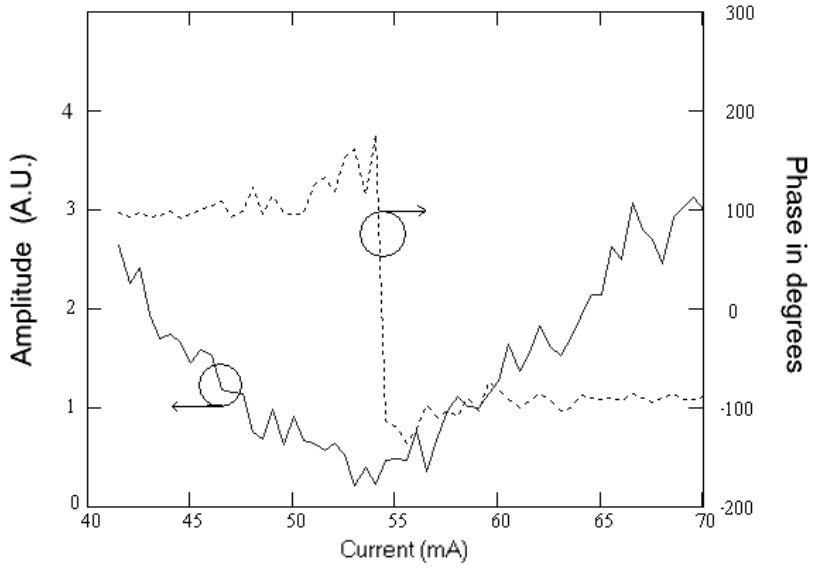

Figure 8. Measured amplitude and phase of the voltage modulation at the laser, versus the current injection, when a modulated light from a tunable laser is injected. A clear transition in the phase indicates the transparency current.

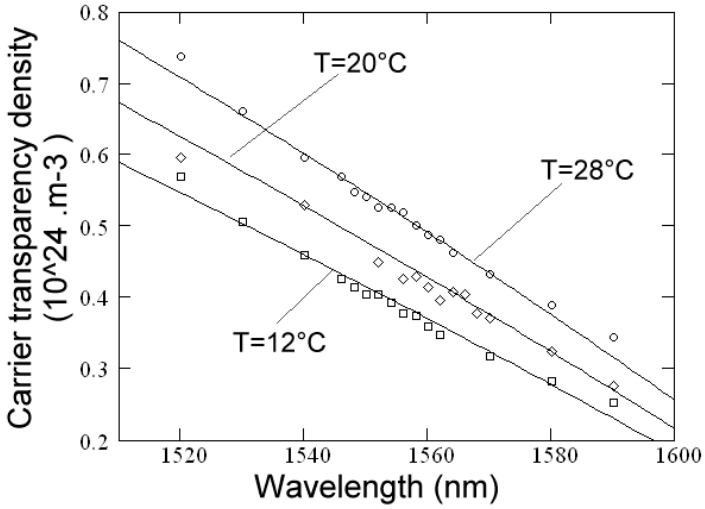

Figure 9. Measured transparency carrier, recalculated in carrier densities, as function of the wavelength (at the temperatures of 12, 20 and 28°C).

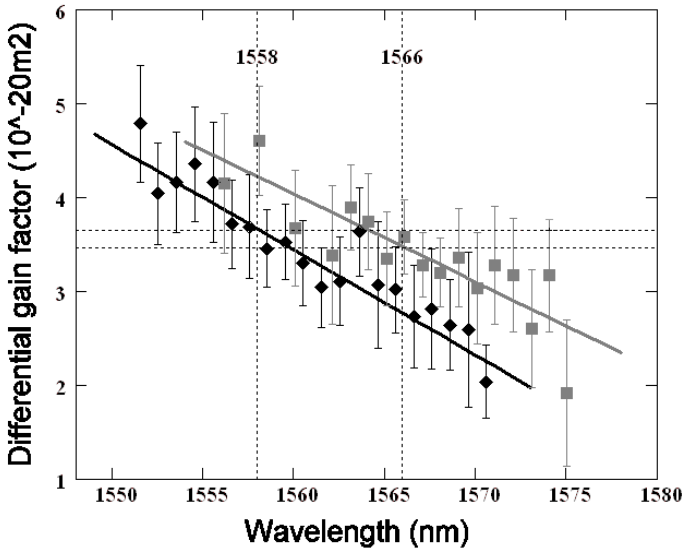

Figure 10. The differential gain parameter $\alpha N\ (\cdot 10^{-20}.m^2)$ as a function of the wavelength and for the temperatures T = 16°C (black diamonds) and T = 28°C (grey squares). Wavelengths at which the device starts lasing for the two temperatures (the maximum of the gain) is indicated.

References

1. B.W. Hakki and T. Paoli, “Gain spectra in GaAs double heterostructure injection lasers”, J. Appl. Ph., vol.46, no. 3, 1299-1305 (1975)
2. D.T. Cassidy, “Technique for measurement of the gain spectra of semiconductor diode lasers”, J. of Appl. Ph. vol.56, no.11, 3096-3099 (1984)
3. H. Wang and D.T. Cassidy, “Gain Measurement of Fabry-Pérot Semiconductor Lasers Using a Non-Linear Least-Squares Fitting Method”, IEEE J.Q.E, vol.41, no.4, (2005)
4. E.I. Gordon “optical maser oscillators and noise” Bell Syst. Tech. J. Vol. 43 pp 507-539, 1964.
5. J. Hader, J.V Moloney, S.W. Koch, “Microscopic theory of gain, absorption, and refractive index in semiconductor laser materials-influence of conduction-bandnon parabolicity and Coulomb-induced intersubband coupling” Quantum Electronics, IEEE Journal of Vol. 35, Issue 12, pp. 1878-1886, 1999.
6. T.A. DeTemple, C.M. Herzinger, “On the semiconductor laser logarithmic gain-current density relation” IEEE J.Q.E. vol 39. 1993 pp 1246-1252
7. W. H. Guo, Y. Z. Huang, C. L. Han, and L. J. Yu, “Measurement of gain for Fabry–Pérot semiconductor lasers by the fourier transform method with a deconvolution process,” IEEE J.Q.E. , vol. 39, no.6 , 716–721, (2003)
8. L. Occhi, L. Schares and G. Guekos, “Phase Modelling Based on the α- Factor in Bulk Semiconductor Optical Amplifiers”, IEEE J.S.T.Q.E, vol.9, no.3, (2003)
9. T. Durhuus, B. Mikkelsen and K.E. Stubkjaer, “Detailed Dynamic Model for Semiconductor Optical Amplifiers and Their Crosstalk and Intermodulation Distortion”, J.L.T. vol.10, no.8, (1992)